法の 3 乗に比例するため，マシンの小型化にはスケーリング則の制限を受けないことを明らかにした。

（平成 17 年 11 月 25 日受付，平成 18 年 6 月 6 日再受付）

文　献

(1) M. Esashi : "Physics of the Micro World and Micromachines", *J. Rob. Soc. Jpn.*, Vol.14, No.8, pp.1086-1089 (1996) (in Japanese)
江刺正喜：「微小世界の物理学とマイクロマシン」，日本ロボット学誌, **14**, 8, pp.1086-1089 (1996)

(2) I. Shimoyama : "Scale Effects in Microrobots", *J. Rob. Soc. Jpn.*, Vol.14, No.8, pp.1106-1108 (1996) (in Japanese)
下山　勲：「マイクロロボットのスケール効果」，日本ロボット学誌, **14**, 8 pp.1106-1108 (1996)

(3) M. Sendoh, K. Shimazaki, K. Ishiyama, M. Inoue, and K. I. Arai : "Swimming Properties of Spiral-Type Magnetic Micro-machines", *J. Magn. Soc. Jpn.*, Vol.23, No.4-2, pp.1657-1660 (1999) (in Japanese)
仙道雅彦・島崎克彦・石山和志・井上光輝・荒井賢一：「スパイラル形状を基本とした泳動型磁気マイクロマシンの泳動特性」，応用磁気学誌, **23**, 4-2, pp.1657-1660 (1999)

(4) M. Tomie, A. Takiguchi, T. Honda, and J. Yamasaki : "Turning Performance of Fish-Type Microrobot Driven by External Magnetic Field", *IEEE Trans. Magn.*, Vol.41, No.10, pp.4015-4017 (2005)

(5) K. I. Arai, W. Sugawara, K. Ishiyama, T. Honda, and M. Yamaguchi : "Fabrication of small flying machines using magnetic thin films", *IEEE Trans. Magn.*, Vol.31, No.6, pp.3758-3760 (1995)

(6) N. Miki and I. Shimoyama : "Soft-Magnetic Rotational Microwings in an Alternating Magnetic Field Applicable to Microflight Mechanisms", *IEEE J Microelectromec. Syst.*, Vol.12, No.2, pp.221-227 (2003)

(7) K. Ishiyama, M. Sendoh, A. Yamazaki, and K. I. Arai : "Swimming micro-machine driven by magnetic torque", *Sens. Actuators. A*, Vol.91, No.1-2, pp.141-144 (2001)

(8) T. Kambe : "Fluid Dynamics", Shokabo (1995) (in Japanese)
神部　勉：「流体力学」，裳華房 (1995)

(9) A. Yamazaki, M. Sendoh, K. Ishiyama, T. Hayase, and K. I. Arai : "Three-Dimensional Analysis of Swimming Properties of the Spiral-Type Magnetic Micro-Machine", *Sens. Actuators. A*, Vol.105, No.1, pp.103-108 (2003)

(10) A. Yamazaki, M. Sendoh, K. Ishiyama, K. I. Arai, R. Kato, M. Nakano, and H. Fukunaga : "Wireless Micro Swimming Machine With Magnetic Thin Film", *JMMM*, Vol.272-276, No.4, pp.e1741-e1742 (2004)

(11) M. Sendoh, A. Yamazaki, K. Ishiyama, K. I. Arai, and M. Inoue : "Wireless Controlling of the Swimming Direction of the Spiral-Type Magnetic Micro-Machines", *Trans. IEE Japan*, Vol.120-A, No.3, pp.301-306 (2000-3) (in Japanese)
仙道雅彦・山崎　彩・石山和志・荒井賢一・井上光輝：「スパイラル型磁気マイクロマシンのワイヤレス泳動方向制御」，電学論 A, **120**, 3, pp.301-306 (2000-3)

(12) A. Yamazaki, M. Sendoh, K. Ishiyama, K. Morooka, and K. I. Arai : "Fabrication of Magnetic Micro-Machine of Planar Structure", *J. Magn. Soc. Jpn.*, Vol.29, No.2, pp.157-160 (2005) (in Japanese)
山崎　彩・仙道雅彦・石山和志・師岡ケイ子・荒井賢一：「平面型構造の磁気マイクロマシンの試作」，応用磁気学誌, **29**, 2, pp.157-160 (2005)

(13) A. Yamazaki, M. Sendoh, K. Ishiyama, and K. I. Arai : "Wireless Magnetic Micro-Machine of Planar Structure with Magnetic Thin Film", *IEEE Trans. Magn.*, Vol.41, No.10, pp.4021-4023 (2005)

山　崎　　彩

（学生員）2000 年 3 月東北大学工学部電気工学科卒業。2005 年 9 月東北大学大学院工学研究科電気通信工学専攻後期課程修了。同年 10 月東北大学電気通信研究所研究生。現在に至る。

仙　道　雅　彦

（正員）　1999 年 3 月東北大学工学部電気工学科卒業。2002 年 4 月日本学術振興会特別研究員 (DC)。2003 年 3 月東北大学大学院工学研究科電気通信工学専攻後期課程修了。2004 年 4 月東北大学電気通信研究所助手。2005 年 4 月（財）みやぎ産業振興機構研究員。現在に至る。

石　山　和　志

（正員）　1986 年東北大学工学部電気工学科卒業。1988 年 3 月東北大学大学院工学研究科電子工学専攻博士前期課程修了。同年 4 月東北大学電気通信研究所助手。2003 年 1 月東北大学電気通信研究所助教授。現在に至る。

荒　井　賢　一

（正員）　1966 年東北大学工学部電子工学科卒業。1971 年東北大学大学院博士課程修了。同年東北大学助手，電気通信研究所。1975 年東北大学助教授，電気通信研究所・1986 年東北大学教授，電気通信研究所。現在に至る。

日本機械学会論文集(C編)
72巻723号(2006-11)

論文 No. 05-1252

3次元泳動特性解析法を用いたらせん型磁気マイクロマシンの形状設計*

山崎 彩*1, 仙道雅彦*2, 石山和志*3
早瀬敏幸*4, 荒井賢一*1

Design of Spiral-Type Magnetic Micro-machine with Three-Dimensional Analysis of Swimming Properties

Aya YAMAZAKI, Masahiko SENDOH, Kazushi ISHIYAMA*5,
Toshiyuki HAYASE and Ken Ichi ARAI

*5 Research Institute of Electrical Communication, Tohoku University,
2-1-1 Katahira, Aoba-ku, Sendai-shi, Miyagi, 980-8577 Japan

Magnetic micro-machines are driven by a magnetic field. They require no power supply cables, no batteries, and no controlling systems on the machine body. In previous studies, we examined the swimming properties of a spiral-type magnetic micro-machine (outer diameter of 0.1 or 1.5 mm) by the experiment and the analysis. This micro-machine is composed of the body of cylinder and the spiral structure. Pulling the thing and the transportation of the thing are given to the application of the micro-machine. At this time, a big load works in the machine. It is necessary to improve thrust to swim against the drag. In this paper, we examined about the influence that machine shape and a spiral shape give to the swimming properties of micro-machie using the analysis. As machine shapes, the having body (Ref-Type) and no (Head-Type) were examined. As a spiral shape, the blade pitch was examined. It was found that the micro-machine of Head-Type suitable for the micro-machine that pulled the thing because the thrust was large. In the case of Ref-Type with the loading on the machine body, the spiral pitch of the maximum thrust was about 1 mm.

Key Words: Micro-machine, Mechatronics and Robotics, Numerical Analysis, Spiral, Rotational Magnetic Field

1. はじめに

著者らは先の研究において，らせん型磁気マイクロマシンの泳動特性について検討を行ってきた[1]．図1に磁気マイクロマシンの概略図を示す．磁気マイクロマシンは，磁石とらせん形状に加工されたワイヤから構成されている．磁石は直径方向に磁化されているため外部からの回転磁界に同期してマシンは回転する．マシンの回転がらせん部分で推力に変換され，マシンは推進する．磁気マイクロマシンの推進方向は，回転面に対して垂直であるため，回転磁界面の方向を変えることによりマシンの推進方向制御も可能となる[2]．

これまでの研究において，直径0.1～1.5 mmのマイクロマシンと幅広い粘度の液体を用いて，らせん型磁気マイクロマシンが幅広いレイノルズ数条件下(10^{-7}<Re<10^{3})で駆動可能であることを実験と解析により明らかにした[3]–[5]．このような磁気力を駆動源とする磁気マイクロマシンは，ワイヤレスに駆動，制御できることから，生体内を移動する医療用マイクロマシン[6]–[9]や化学分析システム(μTAS, Micro Total Analysis System)等に用いるマイクロポンプ[10]としての応用が考えられる．

マイクロマシンの行う仕事として考えられることは，物をけん引したり，マシンに物を搭載して運搬す

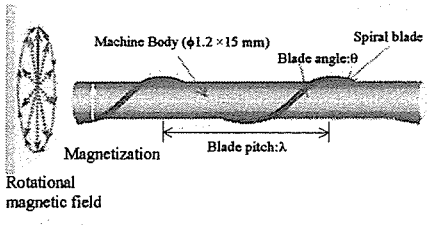

Fig. 1 Schematic view of spiral-type micro-machine (Ref-Type).

* 原稿受付 2005年12月16日.
*1 東北大学電気通信研究所(〒980-8577 仙台市青葉区片平2-1-1).
*2 (財)みやぎ産業振興機構(〒980-0011 仙台市青葉区上杉1-14-2).
*3 正員，東北大学電気通信研究所.
*4 正員，東北大学流体科学研究所.
E-mail: ishiyama@riec.tohoku.or.jp

ることが挙げられる．このようなマシンが推進する際，マシンには推進方向に推力，推進を妨げる方向には流体からの力と外壁との摩擦力，マシンに取り付けた負荷に対する流体からの力などの抵抗力を受ける．この推力と抵抗力が等しいとき，マシンは等速運動を行う．従って，抵抗力に打ち勝ってマシンが推進するためには，推力の大きいマシン形状が求められる．本研究では，先の研究で確立された有限体積法[1]を用いた3次元泳動特性解析法[4]を用いてらせん型マイクロマシンのらせん形状，マシン形状の違いによる泳動特性への影響について検討を行い，マシン設計の指針を得ることを目的とした．

2. 素子構成

マシン形状の違いによる泳動特性への影響を検討するために，図1，2に示すマイクロマシンについて検討を行った．図1は直径1.2 mm，長さ15 mmの円柱形の胴体に高さ0.15 mm幅0.2 mmのらせんを巻きつけた構造である．これをRef-Typeとする．それに対して，図2はRef-Typeの胴体の代わりに，直径1.2 mm，厚さ0.5 mmの円盤をらせんの先端に取り付けた構造である．これをHead-Typeとする．この2種類のマシン形状を用いて，胴体の有無がマシンの泳動に与える影響について検討を行う．らせん形状が泳動特性に与える影響について検討を行うために，図1に示すθをらせん角度，隣り合うらせん間距離λをらせんピッチと定義し，らせん角度θを21，30，38，46，58，72°に変化させて検討を行った．このとき，マシン胴体径1.2 mm，マシン長さ15 mm一定とする．さらに図3に示すように同じらせん角度のらせんを多条巻きし，同一らせん角度において隣り合うらせん間距離を変化させてらせんピッチの影響について検討を行った．検討を行ったらせん角度θ，らせんピッチλ，らせんに沿った全体の長さを表1に示す．また，解析結果の妥当性について検討を行うために，図4 (a)，(b)に示すようにRef-TypeとHead-Typeのマイクロマシンを作製し，実験を行った．Ref-Type，Head-Typeにはそれぞれϕ1.2 × 15 mmのNdFeB磁石(残留磁束密度：1 T)，ϕ1.2(0.35) × 0.55 mmのSmFeN磁石(残留磁束密度：0.64 T)を使用した．らせんには，直径0.15 mmのタングステンワイヤを用いた．

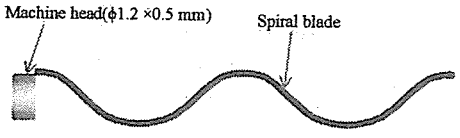

Fig.2 Schematic view of spiral-type micro-machine (Head-Type).

3. マシン形状

3.1 泳動速度特性　図1，2に示すRef-TypeとHead-Typeのマシン形状について解析と実験を行った．らせん角度とらせん条数は46°，1条とした．実験の都合上，Ref-Typeは動粘度0.1 m²/s，Head-Typeは動粘度0.01 m²/sのシリコーンオイルを使用し，印加磁界強度はどちらも12 kA/mである．この2種類の形状を用いて，らせん部分の胴体の有無が泳動特性へ与える影響

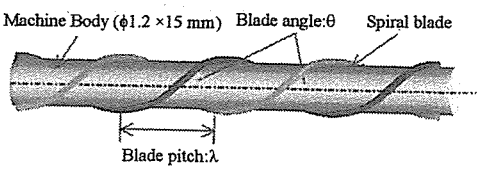

Fig.3 Schematic view of spiral-type micro-machine (Ref-Type, Blade number 2).

Table 1 Size of blade of micro-machine.

Blade angle θ \ Blade number	1	2	3	4	6	8
21°	9.6					
	16.1					
30°	6.4	3.2		1.6		0.8
	17.4	34.8		69.6		139.2
38°	4.8	2.4	1.6	1.2	0.8	0.6
	19.0	38.0	57.0	76.0	114.0	152.0
46°	3.6	1.8	1.2	0.9	0.6	
	21.6	43.2	64.8	86.4	129.6	
58°	2.4	1.2	0.8	0.6		
	28.3	56.6	84.9	113.2		
72°	1.2	Upper: Blade pitch λ (mm)				
	48.5	Lower: Total length of blade (mm)				

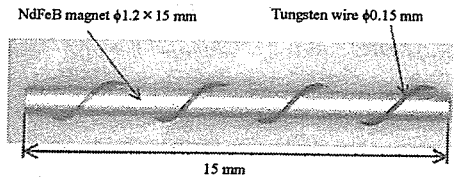

(a) Ref-Type

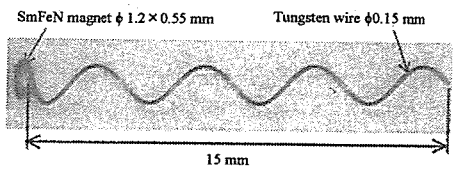

(b) Head-Type

Fig.4 Photograph of spiral-type micro-machine.

について検討を行う．図5にRef-Type，Head-Typeの周波数に対する泳動速度の実験と解析結果を示す．プロットが実験結果，線が3次元泳動特性解析法による解析結果を示す．図中に示す矢印はマシンが回転磁界の同期から外れる周波数であり，以後この周波数を脱調周波数と呼ぶ．Ref-Type，Head-Typeともに脱調周波数以下において周波数に比例して速度は増加した．Ref-Type，Head-Typeそれぞれの1回転当りの推進距離は，0.086，1.2 mmであった．従って，液体の動粘度は異なるが，Head-TypeはRef-Typeより泳動が速いことが明らかとなった．動粘度の影響については次節で述べる．

3.2 推力と抵抗力　Head-Typeの泳動が速い理由について検討を行うために，マシンの速度とマシンに働く推力，抵抗力の関係について解析を行った．解析では，マシンが流体から受ける抵抗力のみを計算した．図6にマシンの泳動速度に対するマシンに働く推力と抵抗力の解析結果を示す．周波数は1 Hzと固定した．実線と破線がRef-Typeの推力と抵抗力，一点鎖線と二点鎖線がHead-Typeの推力と抵抗力である．各マシンの推力と抵抗力が等しい泳動速度が周波数1 Hzにおおけるマシンの泳動速度となる．本章では，2種類の異なる動粘度の液体を用いていることから，液体の動粘度と推力，抵抗力の関係について検討を行う．推力は，推進方向のらせん前後の圧力差によるものである．流体力学における運動量保存則である定常運動でのナビエ・ストークス方程式[12]を式(1)に示す．

$$(V\cdot\nabla)V=-\nabla\left(\frac{p}{\rho_0}\right)+\nu\nabla^2V \qquad (1)$$

ここで，Vは速度，pは圧力，ρ_0は密度，νは動粘度である．本研究では，低レイノルズ数条件下において検討を行っているため，左辺の慣性項は無視できることから，右辺第一項の圧力項は粘度に比例する．従って，らせん前後の圧力差で求められる推力は液体の粘度に比例する．一方，抵抗力はマシン表面のせん断力によるものであり，せん断力[13]は式(2)で表される．

$$\begin{aligned}F_s&=\tau\cdot A\\&=\mu\cdot u\cdot A\end{aligned} \qquad (2)$$

ここで，F_sはせん断力，τはせん断応力，Aは表面積，μは液体の粘度，uは変形速度である．式(2)より，せん断力は液体の粘度に比例するため，抵抗力も粘度に比例する．従って，推力，抵抗力ともに粘度に比例する．これらの結果を踏まえて，マシン形状と泳動特性の関係について検討を行う．Head-Typeの速度が速い要因として，マシン速度0における推力と抵抗力の差が大きいことが考えられる．マシン速度0とは，その場でマシンが回転し，推進していない状態である．Head-Typeは胴体が無いため，らせんの周囲で自由に流れが存在するのに対して，Ref-Typeは胴体により流れが妨げられ，推力が低下したと考えられる．マシン速度0におけるRef-Typeの推力はHead-Typeの約4倍であった．液体の粘度が10倍であることを考慮すると，Head-Typeの推力は大きい．一方，抵抗力は表面積に比例するため，胴体が無く，マシンの表面積が少ないHead-Typeの抵抗力が小さくなった．従って，Head-Typeは推力と抵抗力の差が大きくなったと考えられる．

以上のことから，Head-Typeは抵抗力が少なく，推力が大きいため，推力と抵抗力の等しくなる泳動速度が高速側にシフトしたと考えられる．

3.3 負荷トルク　磁気マイクロマシンは，式(3)で表される磁気トルクにより回転し推進する．

$$T_M=M\cdot H\cdot\sin\delta \qquad (3)$$

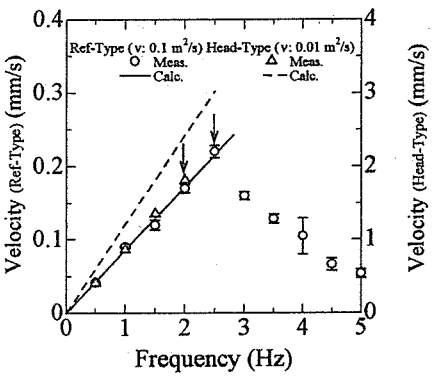

Fig. 5 Relation between frequency and velocity.

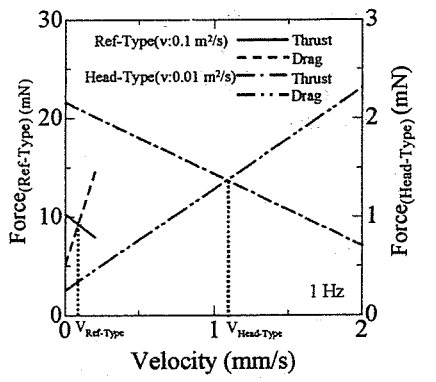

Fig. 6 Relation between velocity of machine and force.

ここで，T_Mは磁気トルク(N m)，Mは磁化(Wb・m)，Hは磁界強度(A/m)，δはMとHの位相差である．回転するマイクロマシンは流体から負荷トルクを受けるため，負荷トルクが磁気トルクを上回ったとき，マイクロマシンは回転磁界の同期から外れる．磁気トルクと負荷トルクが等しい周波数が脱調周波数である．従って，脱調周波数を測定することで，負荷トルクを見積もることが可能となる．表2に，1 Hzにおける負荷トルクの実験と解析結果を示す．実験では，磁界強度を 4～12 kA/m に変化させて脱調周波数を測定し，式(3)を用いて磁気トルクを求め，脱調周波数における負荷トルクとした．求めた負荷トルクから 1 Hz 当りの負荷トルクの平均値を求め実験値とした．実験と解析の結果，負荷トルクはほぼ一致した結果が得られた．負荷トルク Ref-Type と Head-Type の 1 Hz あたりの負荷トルクはそれぞれ，57.4，2.7 μNm / Hz であり，Ref-Type は Head-Type の約 21 倍となった．負荷トルクはせん断力と圧力によるため，推力と同様に，液体の粘度に比例する．従って，液体の粘度が 10 倍であることを考慮しても，Ref-Type の方が負荷トルクは大きい結果が得られた．解析結果より，負荷トルクを胴体 (Cylinder)とらせん(Blade)表面で発生するせん断力，端面で受ける抵抗力(Disk)，らせん前後の圧力差(Pressure)に分けた場合，Ref-Type の負荷トルクの約 72 %は胴体部のせん断力(Shear (Cylinder))である．従って，Head-Type は胴体が無いため，表面積が減少し，負荷トルクが小さくなったと考えられる．

以上の結果より，Head-Type は推力が大きく，負荷トルクが小さい形状であることが示された．

Table 2 Results of load torque.

		Ref-Type	Head-Type
Meas.		55.3	2.6
Analysis	Total	57.4	2.7
	Shear (Cylinder)	40.9	
		72	
	Shear (Blade)	10.4	1.3
		18	48
	Pressure	5.1	0.9
		9	33
	Disk	1.0	0.5
		1	19

Upper: Load torque (μNm)
Lower: Percent (%)

4. らせん形状

4.1 Ref-Type

4.1.1 推進方向成分　図 7 に動粘度 0.1 m²/s，周波数 1 Hz におけるらせんピッチに対するマシンの推力の解析結果を示す．解析の結果，全てのらせん角度においてらせん条数の増加とともに推力は増加し，らせんピッチが約 1 mm 付近で最大値が得られた．推力はらせんのみで発生するので，らせん単位長さ当りに発生する推力を図 8 に示す．らせんピッチが広い場合，隣のらせんの影響が少なく，単位長さ当りの推力値が大きいが，らせんに沿った全体の長さが短いため，全体の推力値が小さい．従って，図 7 においてらせんピッチの減少とともに，らせん全長が長くなるため，全体の推力値が増加したと考えられる．それに対して，らせんピッチが狭い場合，隣のらせんの影響を受け，単位長さ当りの推力値が小さい．従って，全体のらせんの長さは長いが，単位長さあたりの推力が小さいため，図 7 においてらせんピッチの減少とともに，推力値は減少した．以上の結果から，らせんピッチが約 1

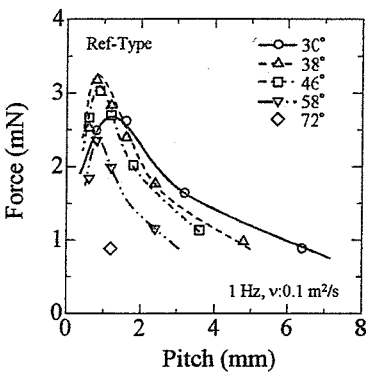

Fig. 7 Relation between blade pitch and force (Ref-Type).

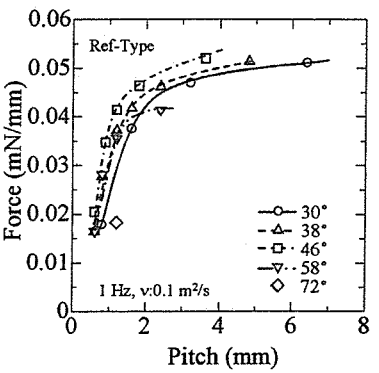

Fig. 8 Relation between blade pitch and force per unit (Ref-Type).

mm付近において，推力の最大値が得られた．図9に動粘度0.1 m²/s，周波数1 Hzにおけるらせんピッチに対するマシンの泳動速度の解析結果を示す．解析の結果，推力の結果と同様にらせん条数の増加とともに泳動速度は速くなり，各らせん角度においてらせんピッチが約1 mm付近において最大値が得られた．従って，推力の大きいらせん形状は泳動速度も速いことが示された．

4.1.2 回転方向成分　図10に動粘度0.1 m²/s，周波数1 Hzにおけるらせんピッチに対する負荷トルクの解析結果を示す．らせん条数の増加に関係なく，らせんピッチが約1 mm以上では，らせん角度によらずほぼ一定の値となり，1 mm以下ではらせんピッチの減少と共に負荷トルクは増加した．負荷トルクの主な要因はマシン表面に働くせん断力によるものであるため，液体の粘度と表面積に比例する．図11にらせんピッチに対するマシン全体の表面積の計算結果を示す．負荷トルクの結果と同様にマシン全体の表面積はらせん角度には依存せず，らせんピッチの減少と共に表面積は増加した．

以上の結果，Ref-Typeはらせん角度によらずらせんピッチが1 mm付近において推力が大きく，負荷トルクが小さい結果が得られた．

4.2 Head-Type

4.2.2 推進方向成分　図12にらせん角度に対する泳動速度の実験と解析結果を示す．○プロットは実験結果，△プロットが解析結果を示す．実験において，磁石部分が下がり傾いた状態で泳動しているため，解析より速度が低下したと考えられる．実験と解析の結果，Ref-Typeと比較して，泳動速度の最大値は30°付近と低角度側にシフトした結果が得られた．図13に推力の解析結果を示す．解析結果より，推力は泳動速度と同様に，30°から45°付近において最大値が得られた．図14に単位長さ当りの推力値と，らせん全長のグラフを示す．Ref-Typeは45°付近から減少していたのに対して，Head-Typeは30°付近より単位長さ当

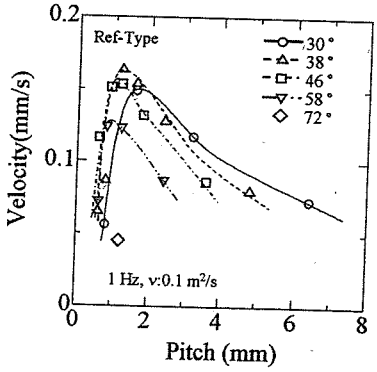

Fig. 9 Relation between blade pitch and velocity (Ref-Type).

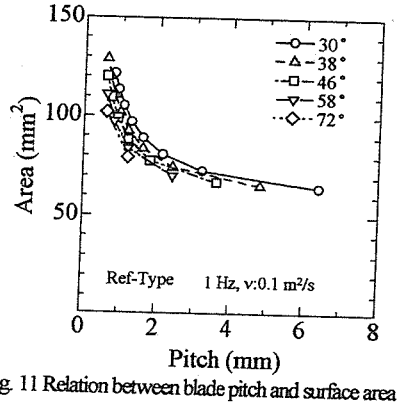

Fig. 11 Relation between blade pitch and surface area of machine (Ref-Type).

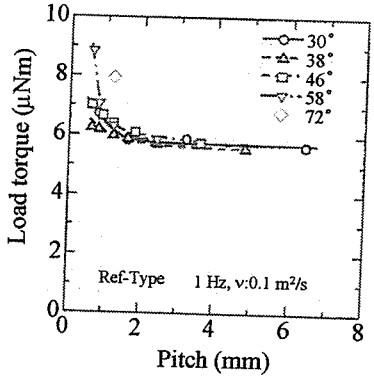

Fig. 10 Relation between blade pitch and load torque (Ref-Type).

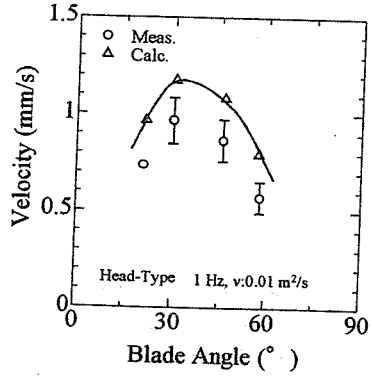

Fig. 12 Relation between blade angle and velocity (Head-Type).

りの推力値は減少している．Head-Type は胴体が無いため，らせんの周辺を自由に流れることができるため，らせん下部においても，流れが存在する．従って，隣のらせんの影響を受けるらせんピッチが狭まり，30° 付近より影響が出始めている．30° 付近までは，らせん全長の増加により推力値は増加し，30° 以上では，らせん全長は増加するが，単位長さ当りの推力値が減少するため推力値が減少したと考えられる．

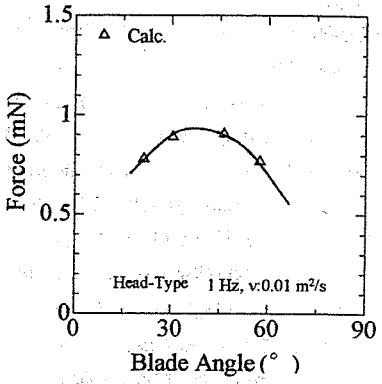

Fig. 13 Relation between blade angle and force (Head-Type).

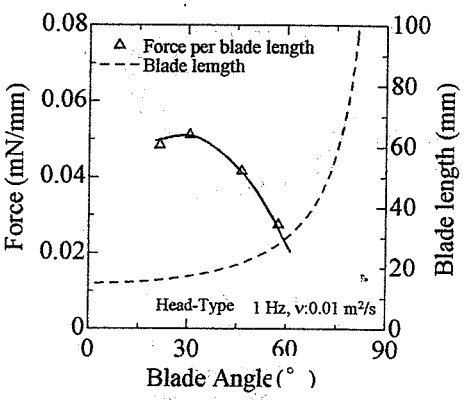

Fig. 14 Relation between blade angle and force per unit (Head-Type).

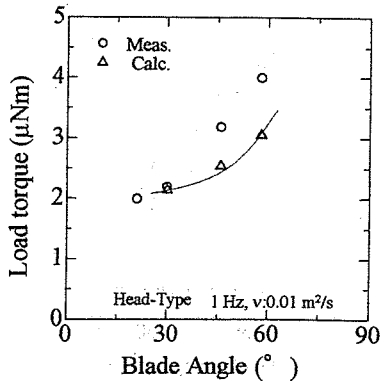

Fig. 15 Relation between blade angle and load torque (Head-Type).

以上の結果より，Ref-Type と比較して，Head-Type は低角度側に推力の最大値がシフトしたため，泳動速度についても 30° 付近において最大値が得られたと考えられる．

4.2.2　回転方向成分　図 15 に負荷トルクの実験と解析結果を示す．実験と解析の結果，負荷トルクはらせん角度の増加に伴い，増加することが示された．Head-Type の負荷トルクの主な要因はらせん表面のせん断力によるものである．従って，らせん表面積の増加に伴い，負荷トルクは増加している．

5. まとめ

3次元泳動特性解析法を用いて磁気マイクロマシンの最適形状について検討を行った．Head-Type のマイクロマシンは，推力が大きい形状であることから，物をけん引するマイクロマシンに適していることが明らかとなった．このときのらせん角度は 30° 付近が推力最大となる．物を搭載できる Ref-Type の場合，らせんピッチはらせん角度によらず，1 mm 付近において推力が最大となった．従って，用途に応じたマシン形状，らせん形状の設計を行う必要がある．

文　献

(1) Sendoh M. et al., Effect of Machine Shape on Swimming Properties of the Spiral-Type Magnetic Micro-Machine. *IEEE Transactions on Magnetics*, Vol. 36, No. 5 (1999) pp. 3688 - 3690.

(2) Sendoh M. et al. Wireless Controlling of the Swimming Direction of the Spiral-Type Magnetic Micro-Machines, *Transaction IEE of Japan*, Vol. 120-A, No. 3 (2000) pp. 301-306.

(3) Ishiyama K. et al., Swimming of Magnetic Micro-Machines under A Very Wide-Range of Reynolds Number Conditions, *IEEE Transactions on Magnetics*, Vol. 37, No. 4 (2001) pp. 2868 - 2870.

(4) Yamazaki A. et al., Three-Dimensional Analysis of Swimming Properties of the Spiral-Type Magnetic Micro-Machine, *Sensors and Actuators A 105* No. 1 (2003) pp. 103-108.

(5) Yamazaki A. et al., Wireless Micro Swimming Machine with Magnetic Thin Film, *Journal of Magnetism and Magnetic Materials* Vol. 272-276 (2004) pp. e1741-e1742.

(6) Chiba. A. et al. *Journal of Magnetics Society of Japan* **29** 343-346, 2005.

(7) Chiba. A. et al. *Journal of Magnetics Society of Japan* **28** 1067-1073, 2004.

(8) Soma. M. et al. *Journal of Magnetics Society of Japan* **29** 594-597, 2004.

(9) Kikuchi K. et al. *IEEE Transactions on Magnetics*, 41, 4012 - 4014, 2005.

(10) Hisatomi. S. et al Micropump with a Spiral-Type Magnetic Micromachine, *Journal of Magnetics Society of Japan* Vol. 29, No. 2 (2005) pp. 76-179.

(11) T. Hayase, et al., Numerical Calculation of Convective Heat Transfer Between Rotating Coaxial Cylinders With Periodically Embedded Cavities, *Journal of Heat Transfer*, Vol. 114 (1992) pp. 589-597.

(12) T. Kambe : "Fluid Dynamics", Shokabo (1995) pp. 38, 52 (in Japanese).

(13) T. Ikui : "Nenseiryutainorikigaku", Rikougakusya (1990) pp. 4 (in Japanese).

厚生労働科学研究費補助金
萌芽的先端医療技術推進研究事業

微細鉗子・カテーテルとその操作技術の開発に関する研究

平成１４年度～１８年度　総合研究報告書

主任研究者　垣添　忠生

平成１９（２００７）年4月１０日

２／２冊

The British Journal of Radiology, 77 (2004), 787–789
DOI: 10.1259/bjr/93367963

Case report

Cervical oesophageal stent placement via a retrograde transgastric route

[1]Y INABA, MD, [2]M KAMATA, MD, [1]Y ARAI, MD, [1]K MATSUEDA, MD, [1]T ARAMAKI, MD and [1]H TAKAKI, MD

Departments of [1]Diagnostic and Interventional Radiology and [2]Radiation Oncology, Aichi Cancer Center, 1-1 Kanokoden Chikusa-ku, Nagoya 464-8681, Japan

Abstract. During attempted oesophageal stent placement in a patient with cervical oesophageal cancer in whom swallowing of even saliva was impossible, transoral access to the cervical oesophagus was unsuccessful. Under ultrasound and fluoroscopy guidance, percutaneous gastric puncture was performed, and using an angiographic catheter and guidewire, access to the oesophagus by a retrograde transgastric route was successfully achieved. The obstructed segment of the oesophagus was traversed. It was then possible to pull the guidewire through the mouth and place an oesophageal stent via an antegrade approach.

The usefulness of metallic stents for the palliation of malignant oesophageal stenoses is well established [1–3]. In general, stent placement in the oesophagus begins with the transoral passage of a guidewire through the oesophageal stenosis under endoscopic or fluoroscopic guidance. Cases are occasionally encountered in which passage of the guidewire is made difficult by the severity of the stenosis. By utilizing angiographic techniques with catheters and guidewires, impassable oesophageal stenoses have become rare.

We recently encountered a patient in whom even swallowing saliva was impossible. Transoral access to the distal cervical oesophagus was not possible due to the severity of the stenosis. As such, we performed a percutaneous gastric puncture, and gained access to the oesophagus by a retrograde transgastric route. It was then possible to pass the guidewire through the stricture into the mouth and place an oesophageal stent via a transoral route antegradely.

Case report

A 55-year-old man with cervical oesophageal cancer associated with tracheal invasion, was treated with external beam radiotherapy (72 Gy) combined with chemotherapy (5-FU and nedaplatin). From the start of these treatments, swallowing of liquids became impaired, and intravenous hyperalimentation was administered. After this treatment the invaded tracheal portion showed improvement, but the patient's dysphagia worsened, and even the swallowing of saliva became impossible. Unfortunately a nasogastric tube for feeding could not be inserted, and under ultrasound guidance the gastric wall was percutaneously punctured with a 23 G needle, the stomach inflated by injecting air into the gastric lumen, and percutaneous gastric puncture performed once again under fluoroscopic guidance using a Cope gastrointestinal suture anchor set (Cook, Bloomington, IN) to create a gastrostomy. However, 1 month later the gastrostomy tube was removed because of a subcutaneous infection around the gastrostomy site.

It was decided to insert an oesophageal self-expanding metallic endoprosthesis, and the cervical oesophagus was approached transorally. Using an angiographic catheter and guidewire, passage through the obstructed portion of the oesophagus was attempted, but the guidewire only entered the associated oesophagotracheal fistula (Figure 1) and did not reach the proximal side of the oesophagus. Endoscopic attempts to traverse the obstruction were also unsuccessful. After treatment of the subcutaneous infection at the earlier gastrostomy site, a repeat percutaneous gastric puncture under ultrasound and fluoroscopy guidance was performed, and a 5 F angiographic sheath (Terumo, Tokyo, Japan) placed in the stomach. An angiographic catheter (5 F Headhunter; Clinical Supply, Gifu, Japan) and guidewire (0.035″ Radifocus; Terumo, Tokyo, Japan) were used to retrogradely cannulate the oesophageal stricture (Figure 1). The guidewire and catheter were then pulled through the mouth. The guidewire was then exchanged for a stiff wire 0.035″ Zebra exchange guidewire (Microvasive/Boston Scientific, Natick, MA). A 24 F Teflon sheath (Cook) was inserted in a transoral, antegrade fashion distal to the oesophageal obstruction, and a covered oesophageal stent (10 cm long covered Ultraflex; Microvasive/Boston Scientific) released proximally, and positioned under fluoroscopy such that its proximal edge did not extend as far as the oral side of the orifice of the oesophagus (Figure 2). The upper edge of the stent after placement was located at the level of the centre of the C6 vertebral body. A nasogastric tube was inserted, and the sheath placed in the stomach was removed. After stent placement the patient felt neither cervical pain nor foreign-body sensation, but experienced pain when attempting to swallow saliva. A follow up contrast study performed on the 4th day after stent placement, showed the stent to be almost completely expanded, and the associated shortening of its long axis resulted in a slightly

Received 9 September 2003 and in revised form 8 December 2003, accepted 3 February 2004.

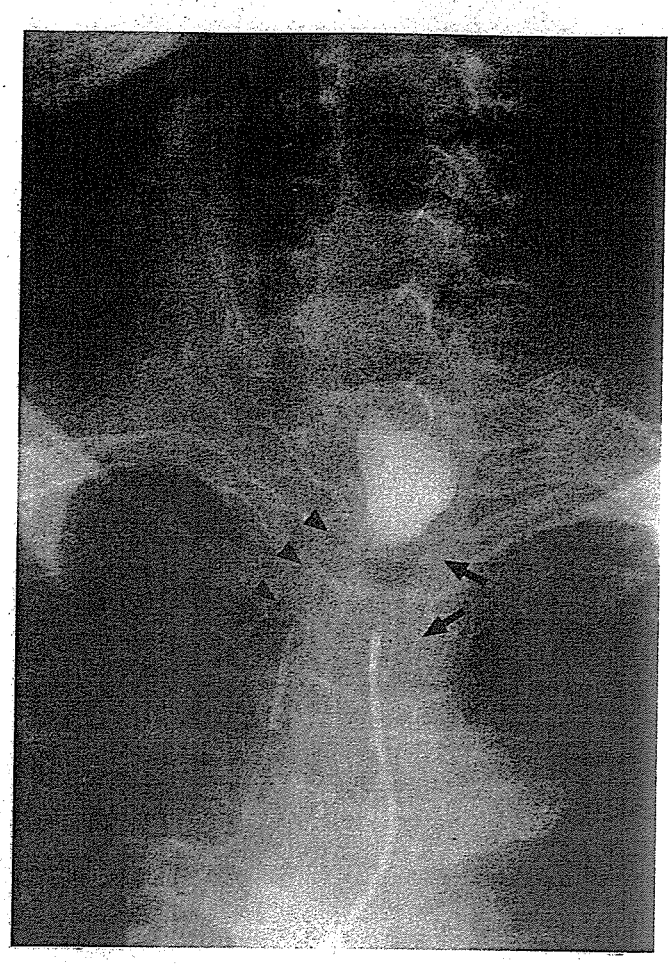

Figure 1. Contrast oesophogogram performed retrogradely via the catheter inserted from the stomach and positioned at the distal edge of the obstructed portion of the oesophagus (arrows). The oesophagus proximal to the stricture and an oesophagotracheal fistula (arrowheads) are visualized.

lower position of the upper edge of the stent. Although only a small volume of contrast material could be swallowed at a time, passage through the stented area was good, and no oesophagotracheal fistula was depicted.

7 days after stent placement the patient was able to swallow smoothly, and oral ingestion of semi-solids became feasible, allowing removal of the nasogastric tube. He died of progressive cancer 5 months after the stent placement, with oral intake continuing to be possible up to the week prior to his death.

Discussion

The use of expandable metallic stents for oesophageal stenoses due to unresectable malignant tumours is now established as valuable palliation, with the rapid amelioration of symptoms in a high proportion of cases. It is minimal invasive and low risk [1–3]. Stent placement is usually possible from the cervical oesophagus to oesophagogastric junction. In the cervical oesophagus there is concern that the more proximally the stent is placed the more marked will be the foreign-body sensation felt by the patient [1]. For this reason, initially stent placement near the oesophageal orifice (within 2 cm of the cricopharyngeus) was considered to be contraindicated [1].

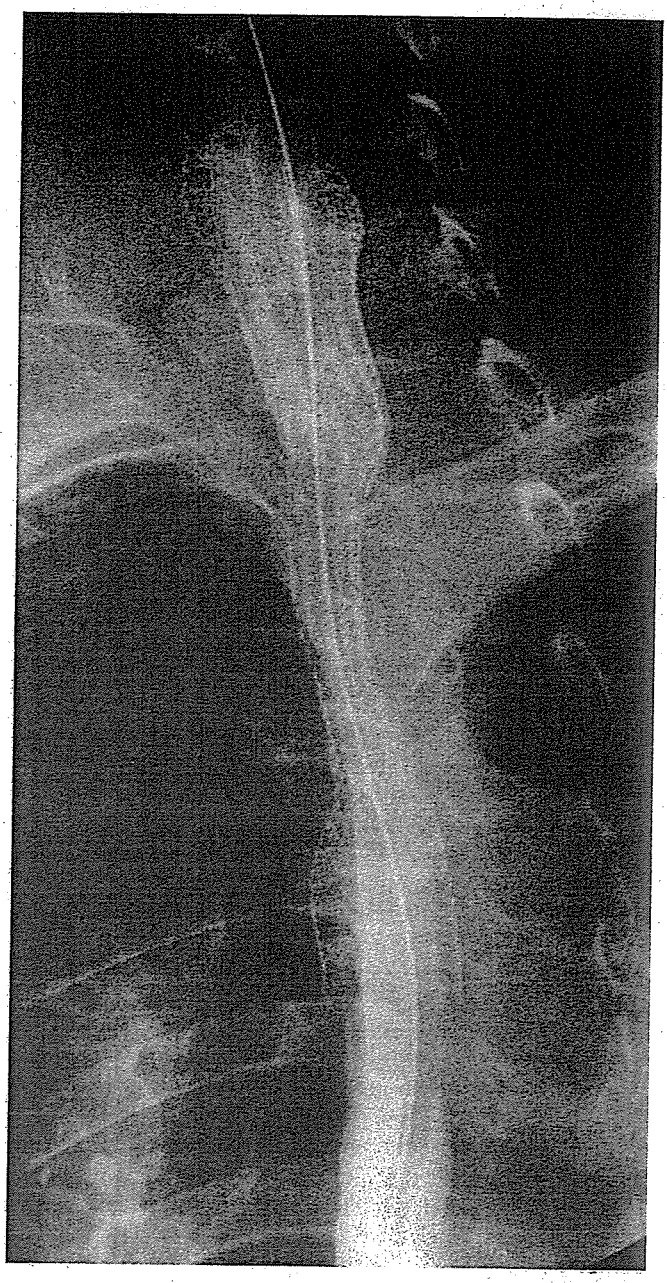

Figure 2. The oesophageal stent inserted via a transoral, antegrade fashion is seen at the level of the oesophageal stricture.

Recently there have been some reports noting an absence of foreign-body sensation problems with stent placement up to the cricopharyngeus [4–7].

Stent placement in the oesophagus is usually via the transoral passage of a guidewire under endoscopic or fluoroscopic guidance through the stenotic portion of the oesophagus. Even in cases in which the severity of the stenosis precludes easy passage, this can usually be achieved by using angiographic technique with angiographic catheters and hydrophilic guidewires. Hitherto we had never experienced a case in which we had to abandon such a procedure because of the unsuccessful passage of a guidewire through the stenosis.

However, in the patient with cervical oesophageal cancer we describe, it was not possible to pass a guidewire transorally through the obstructed portion of the oesophagus. The distance from the cricopharyngeus to the

obstructed portion was approximately 3 cm. Since the radiochemotherapy treatment had successfully reduced the size of the infiltrated portion of the trachea, it is possible that rather than progression of the cancer itself, marked fibrosis associated with the radiotherapy developed.

In cases of vascular obstruction it is not unusual if passage of a guidewire from one direction is difficult, to be able to pass the guidewire from the opposite direction with relative ease [8]. A transgastric retrograde approach was attempted making use of percutaneous gastrostomy technique, and as the stomach was collapsed ultrasound guidance was used. The oesophageal obstruction was traversed retrogradely, enabling a stent to be placed at the stricture. Before the present case, Novak et al reported percutaneous transgastric placement of oesophageal stents [9]. They inserted the 18–24 F delivery system through a gastrostomy, while we placed a 5 F angiographic sheath only in the stomach and pulled a guidewire retrogradely through the mouth, and then inserted the delivery system via an oral route antegradely. After stent placement the 5 F sheath via a transgastric route was removed, but no complications occurred.

Although it is unclear how effective a retrograde approach can be for luminal obstruction when passage from one direction is difficult, in cases in which access can be achieved an approach from both sides should be considered.

References

1. Song HY, Do YS, Han YM, et al. Covered, expandable esophageal metallic stent tubes: experiences in 119 patients. Radiology 1994;193:689–95.
2. Inaba Y, Arai Y, Takeuchi Y, et al. Treatment of malignant gastrointestinal stenoses with expandable metallic stents. J Jpn Soc Angiography Interv Radiol 1997;12:363–9.
3. Siersema PD, Hop WC, van Blankenstein M, et al. A comparison of 3 types of covered metal stents for the palliation of patients with dysphagia caused by esophagogastric carcinoma: a prospective, randomized study. Gastrointest Endosc 2001;54:145–53.
4. Segalin A, Granelli P, Bonavina L, Siardi C, Mazzoleni L, Peracchia A. Self-expanding esophageal prosthesis. Effective palliation for inoperable carcinoma of the cervical esophagus. Surg Endosc 1994;8:1343–5.
5. Bethge N, Sommer A, Vakil N. A prospective trial of self-expanding metal stents in the palliation of malignant esophageal strictures near the upper esophageal sphincter. Gastrointest Endosc 1997;45:300–3.
6. Conio M, Caroli-Bosc F, Demarquay JF, et al. Self-expanding metal stents in the palliation of neoplasms of the cervical esophagus. Hepatogastroenterology 1999;46:272–7.
7. Macdonald S, Edwards RD, Moss JG. Patient tolerance of cervical esophageal metallic stents. J Vasc Interv Radiol 2000;11:891–8.
8. Takeuchi Y, Arai Y, Kasahara T, Inaba Y, Shindo J, Kumada T. Technical aspects of venous stenting in high-grade stenoses using a long guidewire between dual venous access sites. Eur Radiol 2000;10:167–9.
9. Novak Z, Coldwell DM, Mitchell RD, Ryu RK, Kandarpa K. Percutaneous transgastric placement of esophageal stents. J Vasc Interv Radiol 1999;10:428–30.

Primary Mediastinal Lymphoma

Characteristic Features of the Various Histological Subtypes on CT

Ukihide Tateishi, MD, PhD, Nestor L. Müller, MD, PhD,† Takeshi Johkoh, MD, PhD,‡ Yasushi Onishi, MD,§ Yasuaki Arai, MD, PhD,* Mitsuo Satake, MD,* Yoshihiro Matsuno, MD, PhD,‖ and Kensei Tobinai, MD, PhD§*

Objective: To assess the characteristic features of the primary mediastinal lymphoma (PML) on CT and to test the relationship between CT findings and the likelihood of the 3 most common subtypes (Hodgkin lymphoma [HL], mediastinal diffuse large B-cell lymphoma [Med-DLBCL], and precursor T-cell lymphoblastic lymphoma [T-LBL]).

Methods: Sixty-six consecutive patients with pathologically proven PML including 29 patients with HL, 21 with Med-DLBCL, and 16 with T-LBL underwent CT prior to therapy. CT scans were independently reviewed by 2 radiologists who were blinded to the pathologic diagnosis for the following considerations: pattern of involvement (i.e., morphologic features, mass size, and contrast enhancement pattern), and ancillary findings at other sites including neck, abdomen, and pelvis. Interobserver agreement was measured by Kappa statistics, and independent predictors were calculated using multiple logistic regression analysis for determining the likelihood of the subtypes based on CT.

Results: Characteristic features of HL included irregular contour of the anterior mediastinal mass (20 of 29, 69%) and high prevalence of associated mediastinal lymphadenopathy (28 of 29, 97%). Characteristic features of Med-DLBCL included regular contour (14 of 21, 67%) and absence of cervical and abdominal lymphadenopathy (0 of 21). Characteristic features of T-LBL included regular contour (12 of 16, 75%) and high prevalence of cervical (9 of 16, 56%) and abdominal (6 of 16, 38%) lymphadenopathy and splenomegaly (11 of 16, 69%). CT findings independently associated with increased likelihood of HL were surface lobulation ($P < 0.01$), the absence of vascular involvement ($P < 0.01$), or pleural effusion ($P < 0.05$). The presence of vascular involvement was associated with increased likelihood of Med-DLBCL ($P < 0.001$). Furthermore, CT findings including the presence of cervical lymph nodes or inguinal lymph nodes ($P < 0.001$), the presence of pericardial effusion ($P < 0.05$), and the absence of surface lobulation ($P < 0.05$) were significantly associated with the likelihood of T-LBL.

Conclusion: The various histologic subtypes of PML have characteristic manifestations in the neck, chest, and abdomen, which allow their distinction on CT.

Key Words: malignant lymphoma, mediastinal tumor, computed tomography

(*J Comput Assist Tomogr* 2004;28:782–789)

Malignant lymphoma that involves mainly or exclusively the mediastinum at initial presentation (primary mediastinal lymphoma: PML) is a relatively common condition seen in patients of all ages.[1–4] Most cases are due to 1 of 3 histologic subtypes: Hodgkin lymphoma (HL), mediastinal diffuse large B-cell lymphoma (Med-DLBCL), and precursor T-cell lymphoblastic lymphoma (T-LBL). Distinction of the specific histologic subtype is important as it influences treatment and prognosis.[5–12] Because the specific diagnosis should be confirmed by immunohistochemical analysis and hence requires large tissue samples, it is not always easy to make a confident diagnosis on biopsy specimens.[7–10]

There is a sizable body of literature examining the distribution of nodes or masses in lymphoma.[13–27] However, there is limited information on the characteristic manifestations of the various subtypes of PML and the potential value of CT in the differential diagnosis. CT has been increasingly used for the evaluation of patients with suspected or proven lymphoma. It allows for accurate staging of the disease and follow-up of the therapeutic response.[15–23] The purpose of the present study was to assess the characteristic features of the various histologic subtypes of PML and the diagnostic accuracy of CT evaluation for a specific histologic subtype.

MATERIALS AND METHODS

Patients

Sixty-six cases of PML were registered in the radiologic files of our institute. Clinical details and follow-up information including the presence or absence of recurrence were reviewed retrospectively by a hematologic oncologist who was one of the authors. Our institutional review board does not require its approval or patient informed consent for this type of review. The study included 45 men (mean age 38.4 years, range 16 to 84 years) and 21 women (mean age 34.1 years, range 13 to 63 years). All patients underwent uniform staging that included a physical examination, blood cell counts, routine blood

From the *Division of Diagnostic Radiology, National Cancer Center Hospital, Tokyo, Japan; †Division of Hematologic Oncology, National Cancer Center Hospital, Tokyo, Japan; ‖Division of Pathology, National Cancer Center Hospital, Tokyo, Japan; †Department of Radiology, University of British Colombia and Vancouver Hospital and Health Sciences Centre, Canada; and ‡Department of Medical Physics, Osaka University Graduate School of Medicine, Osaka, Japan.

Reprints: Ukihide Tateishi, MD, PhD, Division of Diagnostic Radiology, National Cancer Center Hospital, Tsukiji, Chuo-Ku, 104-0045, Tokyo, Japan (E-mail: utateish@ncc.go.jp).

chemistries, and bone marrow aspiration. Clinical features, International Prognostic Index (IPI) scores,[28] and clinical stages were recorded.

Histopathologic confirmation of definite diagnosis in all patients was obtained by core needle or excisional biopsy. Biopsy sites included the anterior mediastinal mass in 33 patients, cervical lymph node in 25, and both in 8. Fifty-four patients (82%) were confirmed by the initial biopsy alone and the other 12 patients (18%) underwent subsequent biopsy because of insufficient initial sample.

Immunohistochemical studies to determine histologic subtype were performed in all biopsy specimens. According to a recent classification system[29] devised by the World Health Organization (WHO), 29 patients had classic HL, 21 had Med-DLBCL, and 16 had T-LBL. The presence or absence of nodal involvement in each suspected lesion was determined at biopsy in 36 sites and the remaining with a combination of imaging findings and clinical follow-up. Extranodal involvement in the abdomen confirmed by endoscopic, needle, or excisional biopsy included stomach (n = 1), kidney (n = 1), and spleen (n = 1).

The histopathologic findings were reviewed by an experienced pathologist who was one of the authors. Chart, review of histologic specimens, and patient file reviews were

TABLE 1. CT Findings in Patients With PML and the Other Common Nonlymphomatous Diseases

Disease	PML	Thymoma	Thymic cancer	GCT	SCLC
No. of patients	66	19	26	13	12
Male/female	45/21	8/11	18/8	13/0	9/3
Age (mean ± SD) (y)	37.0 ± 14.9	55.6 ± 12.2	58.4 ± 11.6	26.5 ± 5.4	64.5 ± 8.3
Age range (y)	13–84	29–74	24–74	18–38	51–78
Tumor margins*					
Well-defined margins	39 (59)	18 (95)	22 (85)	1 (8)	0
Ill-defined margins	27 (41)	1 (5)	4 (15)	12 (92)	12 (100)
Size of main mass (mean ± SD) [cm]	8.9 ± 3.0	5.2 ± 1.8	7.2 ± 2.4	11.6 ± 2.2	5.6 ± 1.6
Presence of surface lobulation	31 (47)	7 (37)	19 (73)	0	12 (100)
Presence of vascular encasement	21 (32)	1 (5)	20 (77)	7 (54)	2 (17)
Presence of chest wall invasion	10 (15)	0	13 (50)	3 (23)	0
Presence of cutaneous involvement	3 (5)	0	0	0	0
Presence of lung invasion†	11 (17)	0	0	0	NA
Presence of nodal involvement					
Cervical lymph node (superficial)†	10 (15)	0	0	0	0
Cervical lymph node (deep)§	18 (27)	0	0	0	0
Submandibular lymph node	1 (2)	0	0	0	0
Submental lymph node	2 (3)	0	0	0	0
Parotid lymph node	2 (3)	0	0	0	0
Supraclavicular lymph node	11 (17)	0	0	0	10 (83)
Mediastinal lymph node§	50 (76)	0	12 (46)	1 (8)	12 (100)
Hilar lymph node†	12 (15)	0	2 (8)	2 (15)	12 (100)
Axillary lymph node§	12 (15)	0	0	0	0
Celiac lymph node	4 (6)	0	0	0	0
Paraaortic lymph node§	12 (15)	0	0	0	0
Mesenteric lymph node	2 (3)	0	0	0	0
Iliac lymph node	1 (2)	0	0	0	0
Inguinal lymph node*	5 (8)	0	0	0	0
Presence of pleural effusion	26 (39)	2 (10)	8 (31)	5 (38)	5 (42)
Presence of pericardial effusion*	24 (36)	0	4 (15)	3 (23)	3 (25)
Hepatomegaly	2 (3)	0	0	0	0
Splenomegaly§	13 (20)	0	0	0	0
Presence of metastasis					
Lung metastasis§	0	0	5 (19)	7 (54)	3 (25)
Liver metastasis§	0	0	1 (4)	1 (8)	5 (42)
Splenic metastasis	1 (2)	0	0	1 (8)	0
Adrenal metastasis	0	0	0	0	1 (8)
Presence of pleural dissemination	13 (20)	2 (10)	6 (23)	2 (15)	2 (17)

Data in parentheses are percentages.
*$P < 0.05$, †$P < 0.01$, §$P < 0.0001$.
PML, Primary mediastinal lymphoma; GCT, germ cell tumor; SCLC, small cell lung cancer; NA, not applicable.

conducted independently of the CT analysis. All patients with PML underwent treatment, which included chemotherapy and radiotherapy for HL, chemotherapy and/or radiotherapy for Med-DLBCL, and chemotherapy and radiotherapy for T-LBL. Follow-up documentation was reviewed for any evidence of misdiagnosis at any repeat imaging examinations, biopsies, laboratory tests, or on the basis of ongoing symptoms and signs. At the time of this review, there has been no case of initial misdiagnosis.

To determine whether or not CT findings can accurately differentiate PML from the other common nonlymphomatous diseases, a total of 70 patients including thymoma (n = 19), thymic cancer (n = 26), germ cell tumor (n = 13), and small cell lung cancer (n = 12) were also enrolled in this study (Table 1). Selective criteria of these cases were 1) main anterior mediastinal mass identified on CT at presentation, 2) definite diagnosis confirmed by the pathologic observation of main mass, and 3) CT examination performed prior to therapy. These cases were selected from the radiologic files of our institute, and clinical details and follow-up information were also reviewed retrospectively by a radiologist who was one of the authors.

Imaging Studies

CT was performed on a 4-row multidetector scanner (Aquilion V-detector, Toshiba Medical Systems, Tokyo, Japan). The images were obtained at 240–260 mAs, 120 kV, 7-mm collimation sections overlapped in 3.5-mm intervals from the level of the orbit to the proximal femur, and a pitch of 10.5. All patients received 150 mL of nonionic intravenously administered contrast material at 3.0 mL/s with a power injector (Autoenhance A-250; Nemoto-kyorindo, Tokyo, Japan) after a 60-second delay. All patients also received 200–300 mL of sterile water orally prior to CT examination.

Image Analysis

Two experienced radiologists who had knowledge of the diagnosis of primary mediastinal lymphoma but were blinded to histologic subtypes and any clinical information other than patient age and sex independently reviewed the CT images on hard copies. The 2 readers analyzed the images for tumor size, tumor margins (well defined or ill defined), and presence of surface lobulation. The presence of a single mass or confluent lymphadenopathy in the anterior mediastinum was analyzed as representing the primary tumor mass and the measurement based on the short axis diameter. The contrast enhancement of the primary lesions was compared with that of normal muscle. The tumor was considered homogeneous if it enhanced to the same degree throughout. The patterns of local invasion were recorded: encasement of vascular structures, chest wall invasion, cutaneous involvement, and lung invasion. Vascular encasement was considered present when there was circumferential narrowing or complete obstruction of the superior vena cava or brachiocephalic vein by tumor. The presence or absence of lymphadenopathy, pleural effusion, pericardial effusion, and other organ involvement were also evaluated. Nodes were considered enlarged when their short axis diameter was greater than 10 mm. Hepatomegaly and splenomegaly were considered present when the liver and spleen were greater than 13 cm and 12 cm in longitudinal diameter at the midclavicular line, respectively.[29]

Statistical Analysis

Kruskal-Wallis test was used to compare the clinical variables and all CT findings in the 3 histologic subtypes of PML and the other common nonlymphomatous disorders. Student t test was used to compare mean tumor size of the mediastinal mass. The interobserver variation in the interpretation of all CT findings was analyzed using Kappa statistics. The interobserver agreement was classified as follows: poor, k = 0–0.20; fair, k = 0.21–0.40; moderate, k = 0.41–0.60; good, k = 0.61–0.80; and excellent, k = 0.81–1.00. The relationship between CT findings and the likelihood of the histologic subtypes was tested for independent predictors using multiple logistic regression analysis, which determined the odds ratio after adjusting for the other variables examined. All P values less than 0.05 were considered to indicate a statistically significant difference.

RESULTS

Statistically significant CT findings which have possibility of discriminating PML from the other common nonlymphomatous diseases were tumor margins, the presence of lung invasion, involvement of various lymph nodes including cervical (superficial and deep), mediastinal, hilar, axillary, paraaortic, inguinal lymph nodes, the presence of pericardial effusion, splenomegaly, the presence of lung metastasis, and liver metastasis. Patient demographics are listed in Table 2. Patients with Med-DLBCL were slightly older (mean age ± SD: 46.4 ± 18.0) than those with HL (34.6 ± 10.7) or T-LBL (30.6 ± 12.4) ($P < 0.01$). No other significant difference was seen in patient demographics between the 3 subtypes of PML.

TABLE 2. Demographic and Clinical Data in Patients With PML

Disease	HL	Med-DLBCL	T-LBL
No. of patients	29 (44)	21 (32)	16 (24)
Age (mean ± SD) (y)	34.6 ± 10.7	46.4 ± 18.0	30.6 ± 12.4*
Age range (y)	19–57	23–84	13–64
Gender			
Male	17 (59)	15 (71)	13 (81)
Female	12 (41)	6 (29)	3 (19)
IPI score			
Low	23 (79)	12 (57)	6 (38)
Low–intermediate	5 (17)	2 (10)	8 (50)
Intermediate–high	0	5 (24)	1 (6)
High	1 (3)	2 (10)	1 (6)
Clinical stage			
I	7 (24)	11 (52)	2 (13)
II	15 (52)	3 (14)	2 (13)
III	4 (14)	1 (5)	3 (19)
IV	3 (10)	6 (29)	9 (56)

Data in parentheses are percentages. Significant difference is found in the mean age between Med-DLBCL and T-LBL (*$P < 0.01$).

HL, Hodgkin lymphoma; Med-DLBCL, mediastinal diffuse large B-cell lymphoma; T-LBL, T-cell lymphoblastic lymphoma; IPI, International Prognostic Index.

Enlargement of cervical lymph nodes was seen more commonly in T-LBL (10 of 16 patients, 63%) than in HL (9 of 29 patients, 31%) ($P < 0.05$) and was not present in any of the patients with Med-DLBCL (Fig. 1). Of the cervical nodes, deep cervical nodes were affected more frequently in HL (31% [9 of 29 patients]) or T-LBL (56% [9 of 16 patients]) than those in Med-DLBCL (no patients). Superficial nodes were also involved more often in T-LBL (44% [7 of 16 patients]) than in HL (10% [3 of 29 patients], $P < 0.05$). Involvement of supraclavicular lymph nodes was seen more frequently in T-LBL (50% [8 of 16 patients]) compared with that in HL (10% [3 of 29 patients], $P < 0.01$). Submandibular, submental, and parotid lymph nodes were involved only in T-LBL (19% [3 of 16 patients]).

No significant difference was found in the size and margin of the primary lesion between the three histologic subtypes (Table 3). Surface lobulation (Fig. 2) was more common in HL (69% [20 of 29 patients]) than in both Med-DLBCL (33% [7 of 21 patients]) and T-LBL (25% [4 of 16 patients]) ($P < 0.01$, Table 3). The prevalence of vascular involvement including encasement of superior vena cava and left brachiocephalic vein in Med-DLBCL (62% [13 of 21 patients], $P < 0.0001$) and T-LBL (38% [6 of 16 patients],

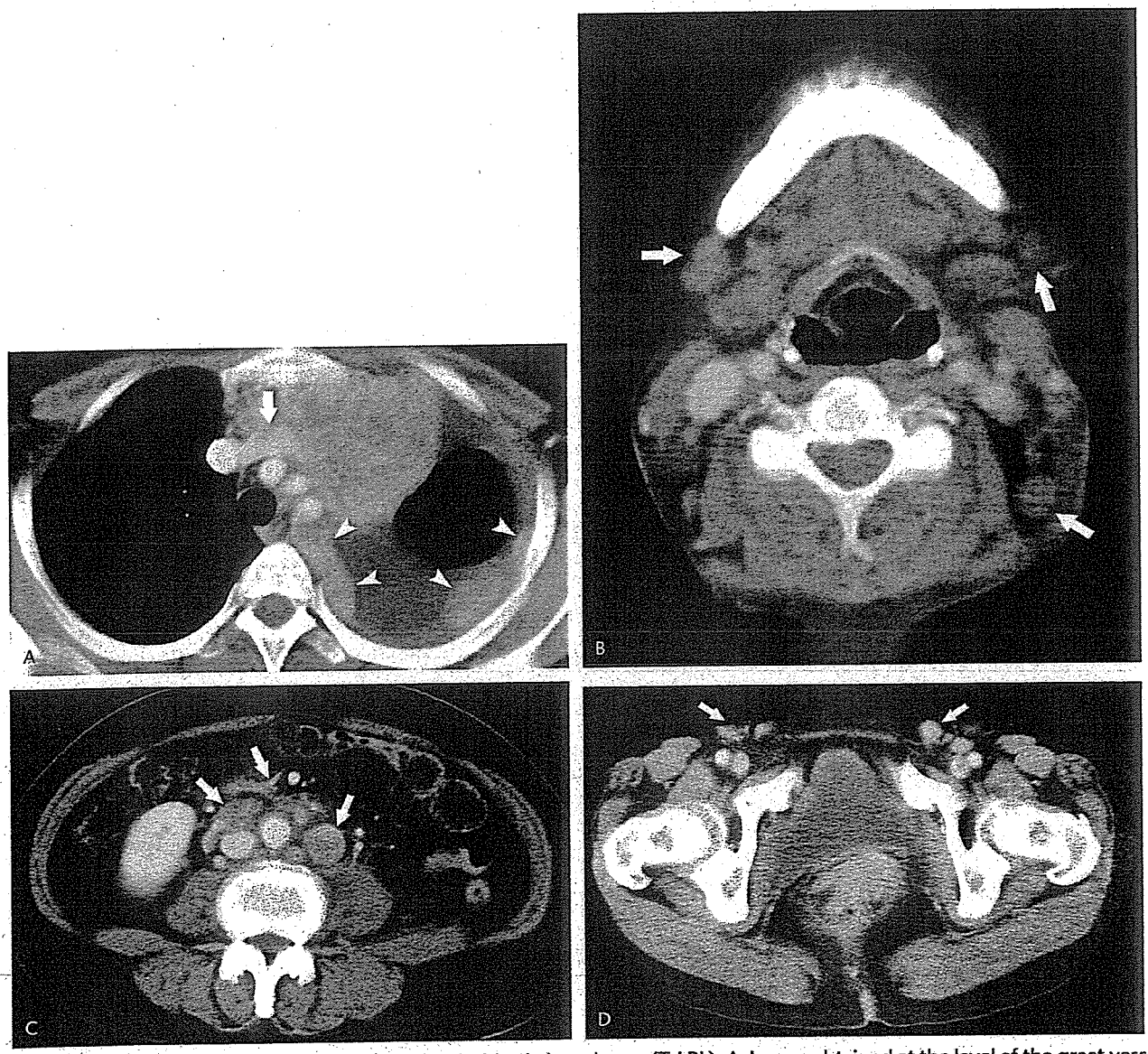

FIGURE 1. Thirty-two-year-old man with T-cell lymphoblastic lymphoma (T-LBL). A, Image obtained at the level of the great vessels shows a large anterior mediastinal mass with encasement and stenosis of the left brachiocephalic vein (arrow). Also noted are left pleural effusion and soft-tissue masses (arrowheads) in the left pleura suggestive of pleural dissemination. B, Image at the level of the upper neck demonstrates several enlarged of cervical nodes (arrows). C, Image at the level of the lower pole of the right kidney shows multiple enlarged paraaortic and mesenteric nodes. D, Image at the level of the inguinal region shows enlarged inguinal lymph nodes (arrows).

TABLE 3. CT Findings in Patients With PML

Disease	HL	Med-DLBCL	T-LBL
No. of patients	29 (44)	21 (32)	16 (24)
Tumor margins			
Well-defined margins	19 (66)	10 (48)	10 (62)
Ill-defined margins	10 (34)	11 (52)	6 (38)
Size of main mass (mean ± SD) (cm)	9.7 ± 2.8	9.7 ± 2.5	10.2 ± 3.3
Presence of surface lobulation*	20 (69)	7 (33)	4 (25)
Presence of vasular encasement†	2 (7)	13 (62)	6 (38)
Presence of chest wall invasion	4 (14)	4 (19)	2 (13)
Presence of cutaneous involvement	0	2 (10)	1 (6)
Presence of lung invasion	8 (28)	2 (10)	1 (6)
Presence of nodal involvement			
Cervical lymph node (superficial)*	3 (10)	0	7 (44)
Cervical lymph node (deep)†	9 (31)	0	9 (56)
Submandibular lymph node	0	0	1 (6)
Submental lymph node‡	0	0	2 (13)
Parotid lymph node‡	0	0	2 (13)
Supraclavicular lymph node§	3 (10)	0	8 (50)
Mediastinal lymph node†	28 (97)	14 (67)	8 (50)
Hilar lymph node‡	10 (34)	1 (5)	1 (6)
Axillary lymph node†	4 (14)	0	8 (50)
Celiac lymph node	3 (10)	0	1 (6)
Paraaortic lymph node*	6 (21)	0	6 (38)
Mesenteric lymph node‡	0	0	2 (13)
Iliac lymph node	0	0	1 (6)
Inguinal lymph node†	0	0	5 (31)
Presence of pleural effusion‡	6 (21)	12 (57)	8 (50)
Presence of pericardial effusion‡	5 (17)	10 (48)	9 (56)
Hepatomegaly‡	0	0	2 (13)
Splenomegaly†	1 (3)	1 (5)	11 (63)

Date in parentheses are percentages.
*$P < 0.01$, †$P < 0.001$, ‡$P < 0.05$, §$P < 0.0001$.
HL, Hodgkin lymphoma; Med-DLBCL, mediastinal diffuse large B-cell lymphoma; T-LBL, T-cell lymphoblastic lymphoma.

$P < 0.05$) was greater than that in HL (7% [2 of 29 patients], Figs. 1 and 2). Complete obstruction of the superior vena cava (SVC syndrome) was present in one of 29 patients with HL (3%), 4 of 21 with Med-DLBCL (19%), and 2 of 16 patients with T-LBL (13%). Forty-one of 66 tumors (62%) showed heterogeneous enhancement on CT, with no significant difference between 3 histologic subtypes.

Enlarged mediastinal nodes distinct from the primary lesion were present more commonly in HL (97% [28 of 29 patients]) than in Med-DLBCL (67% [14 of 21 patients], $P < 0.05$) and T-LBL (50% [8 of 16 patients], $P < 0.0001$, Table 3). Involvement of hilar nodes (Fig. 3) was significantly more common in HL (34% [10 of 29 patients]) compared with Med-DLBCL (5% [1 of 21 patients], $P < 0.05$) and T-LBL (6% [1 of 16 patients], $P < 0.05$). Involvement of bilateral axillary nodes was significantly more common in T-LBL (50% [8 of 16 patients]) than in Med-DLBCL (no patients, $P < 0.0001$) and HL (14% [4 of 29 patients], $P < 0.05$). Pleural effusion (Figs. 1 and 2) was significantly more common in Med-DLBCL (57% [12 of 21 patients], $P < 0.01$) or T-LBL (50% [8 of 16 patients], $P < 0.05$) than in HL (21% [6 of 29 patients]). Of the patients with pleural effusion, tumor cells were confirmed by cytology in 6 of 6 patients with HL (100%), in 5 of 12 with Med-DLBCL (42%), and in 2 of 8 patients (25%) with T-LBL. Pericardial effusion (Fig. 4) was significantly more common in T-LBL (56% [9 of 16 patients], $P < 0.01$) and Med-DLBCL (48% [10 of 21 patients], $P < 0.05$) than in HL (17% [5 of 29 patients]).

Statistically significant CT findings in the abdomen included splenomegaly, and involvement of paraaortic, mesenteric, and inguinal lymph nodes (Table 3). Splenomegaly was present more commonly in T-LBL (63% [11 of 16 patients]) than in HL (3% [1 of 29 patients], $P < 0.0001$) and Med-DLBCL (5% [1 of 21 patients], $P < 0.0001$). Involvement of abdominal paraaortic nodes (Fig. 1) was more common in T-LBL (38% [6 of 16 patients], $P < 0.01$) or HL (21% [6 of 29 patients], $P < 0.05$) than in Med-DLBCL (no patients). Involvement of inguinal (31% [5 of 16 patients]) or mesenteric lymph nodes (13% [2 of 16 patients]) was found only in T-LBL (Fig. 1). Extranodal lesions in the abdomen were proved pathologically in 3 patients. Two patients with Med-DLBCL had mass lesions in the stomach and kidney, and the

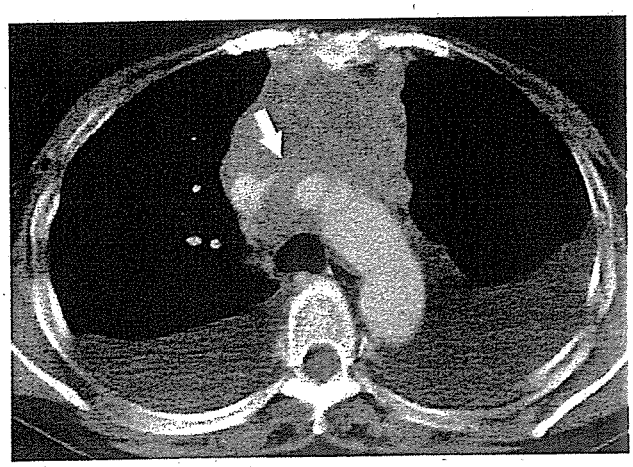

FIGURE 2. Thirty-two-year-old man with mediastinal diffuse large B-cell lymphoma (Med-DLBCL). CT image at the level of the aortic arch demonstrates a large, homogeneous enhancing anterior mediastinal mass without surface lobulation that compresses the left brachiocephalic vein (arrow). Also noted are bilateral pleural effusions.

other patient with HL had focal splenic mass. None of patients with T-LBL had evidence of extranodal involvement on the abdominal CT images.

There was excellent interobserver agreement for CT findings, including morphology and extent of main mass, enhancement pattern, lymph node enlargement, the presence of pleural effusion, pericardial effusion, hepatomegaly, and splenomegaly (Kappa = 0.82–1.00). Multiple logistic regression analysis demonstrated that the CT finding independently associated with increased likelihood of HL was surface lobulation ($P < 0.01$; Table 4), the absence of vascular involvement ($P < 0.01$), or pleural effusion ($P < 0.05$). The presence of vascular involvement was independently associated with increased likelihood of Med-DLBCL ($P < 0.001$, Table 4). In addition, CT findings including the presence of cervical lymph nodes or inguinal lymph nodes ($P < 0.001$; Table 4), the presence of pericardial effusion ($P < 0.05$), and the absence of surface lobulation ($P < 0.05$) were significantly associated with the likelihood of T-LBL.

DISCUSSION

Several studies have described the CT manifestations of PML. The typical presentation consists of an anterior mediastinal mass often associated with enlarged nodes in the middle and posterior mediastinum, and hila.[13–24] The mediastinal mass may involve vascular structures, pericardium, heart, pleura, lung, and chest wall on CT.[13–27] PML often affects extrathoracic sites at the time of diagnosis, particularly abdomen, head, and neck.[28,29]

The current study demonstrates that the different subtypes of PML often have characteristic manifestations that allow their distinction on CT. HL is characterized by the presence of a discrete anterior superior mediastinal mass with surface lobulation. Surface lobulation was present in 69% of patients with HL compared with 33% of patients with

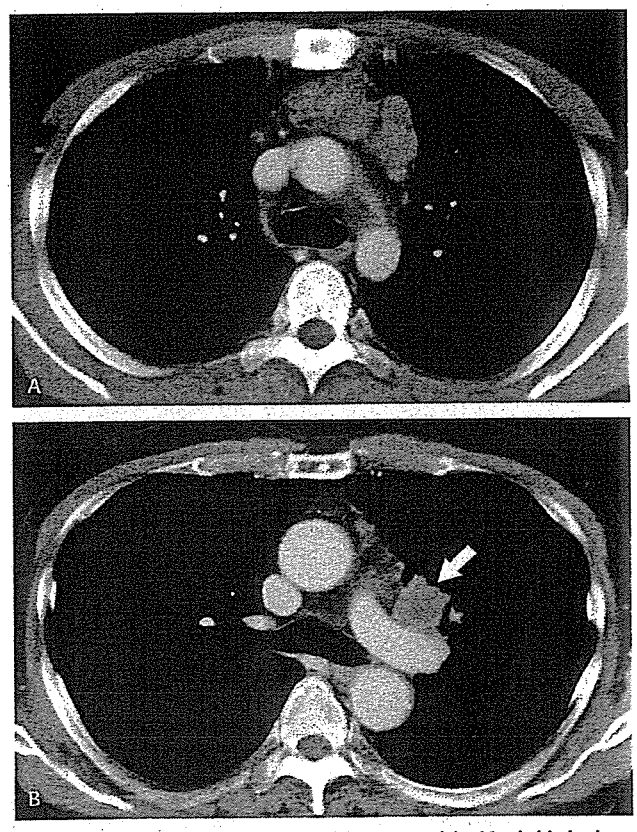

FIGURE 3. Twenty-nine-year-old man with Hodgkin's lymphoma (HL). A, Image at the level of the aortopulmonary window shows anterior mediastinal mass with surface lobulation and heterogeneous enhancement. B, Section obtained at the level of the carina demonstrates enlarged left hilar nodes (arrow).

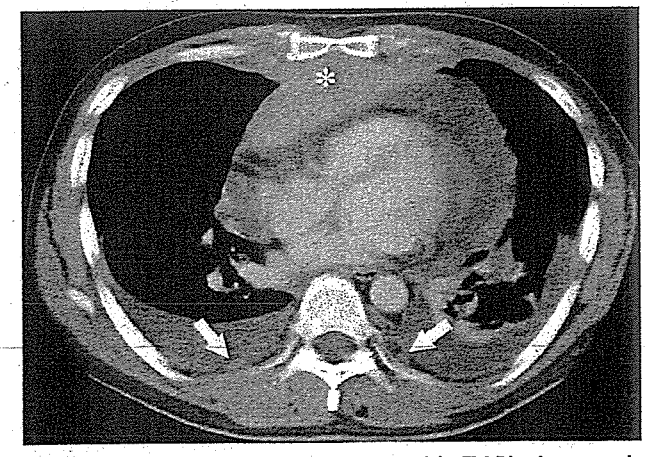

FIGURE 4. Thirty-two-year-old man with T-LBL. Image obtained at the level of the right ventricle shows a large anterior mediastinal mass (asterisk) with marked pericardial effusion. Also noted are pleural effusion bilaterally and soft-tissue nodular dissemination (arrows) in the pleura.

TABLE 4. Relationship Between CT Findings and the Likelihood of the PML Hisologic Subtypes

	CT findings	OR	95% CI	*P*
HL	Presence of surface lobulation	11.9	2.5–56.0	<0.01
	Absence of vascular involvement	11.8	1.9–71.9	<0.01
	Absence of pleural effusion	6.6	1.3–33.2	<0.05
Med-DLBCL	Presence of vascular involvement	7.5	2.3–24.1	<0.001
T-LBL	Presence of cervical or inguinal lymph node	33.9	4.7–244.6	<0.001
	Presence of pericardial effusion	11.4	1.7–77.6	<0.05
	Absence of surface lobulation	7.0	1.2–43.1	<0.05

HL, Hodgkin lymphoma; Med-DLBCL, mediastinal diffuse large B-cell lymphoma; T-LBL, T-cell lymphoblastic lymphoma; OR, odds ratio; CI, confidence interval.

Med-DLBCL and 25% with T-LBL. The surface lobulation of the main mass is due to involvement of multiple nodes and coalescence, a finding previously noted in HL at CT.[13,14] Enlarged nodes elsewhere in the mediastinum were seen in 97% of patients with HL in the current study and less commonly in the other subtypes.

Masses typically exhibit homogeneous soft-tissue attenuation, while large tumors may demonstrate heterogeneity with complex low attenuation representing necrosis, hemorrhage, and cystic degeneration.[20] Sixty-two percent of our cases showed heterogeneous enhancement on CT, with no significant difference between 3 histologic subtypes.

Med-DLBCL typically is initially confined to the mediastinum and contiguous nodal areas without showing extrathoracic disease at presentation.[3,5] Med-DLBCL may present with hematogenous spread to parenchymal organs such as kidney, liver, ovary, adrenal gland, gastrointestinal tract, and central nervous system during disease progression or at recurrence.[3] Extranodal involvement was found on the initial CT assessment and was confirmed by biopsy in 2 of our Med-DLBCL cases, whereas extrathoracic nodal involvement was not found in any of our patients with Med-DLBCL. Some observers consider that Med-DLBCL is a pathologic and clinical entity of non-Hodgkin lymphoma derived from mature thymic B-cells recognized by previous immunophenotypic studies.[30,31] However, the histogenesis is controversial, because Med-DLBCL can result in diffuse nodal involvement in advanced stages.[3,5]

Extrathoracic lymphadenopathy including superficial cervical, supraclavicular, submandibular, submental, parotid, mesenteric, and inguinal nodes, was seen in the majority of patients with T-cell lymphoblastic lymphoma in the present study. Another common finding in T-cell lymphoblastic lymphoma in the current study was the presence of splenomegaly, which was seen in 63% of cases. HL often involved axial lymph nodes including cervical, mediastinal, axillary, and paraaortic regions. However, none of the patients with HL in the current study had submandibular, submental, parotid, mesenteric, and inguinal lymphadenopathy. The low prevalence of nonaxial lymphadenopathy in HL had been recognized in previous studies.[29,32]

Diagnosis of subtypes in all patients was established by core or excisional biopsy in all cases. The ability to classify PML in small samples has improved considerably in the last few years because of progress of pathologic criteria and immunocytochemistry.[33,34] HL is characterized by a large inflammatory cell reaction within a fibrotic stroma, and the diagnosis is established by the identification of Hodgkin and Reed-Sternberg (HRS) cells.[2] Med-DLBCL is composed mainly of large clear cells within a characteristic background of compartmentalized fibrosis.[5] T-LBL is composed of a homogeneous population of immature lymphoblastic cells cytologically similar to acute lymphoblastic leukemia.[8–10] Biopsy provides sufficient information for the diagnosis of and subsequent therapeutic decision to treat patients with PML, because the definitive selection of therapeutic regimen is needed.

Our study has several limitations. It is retrospective and includes a relatively small number of patients. In clinical practice, the differential diagnosis would need to include a variety of other conditions that can present with an anterior mediastinal mass. However, we believe that the study demonstrates that the various histologic subtypes of PML have features on CT that allow distinction in the majority of cases. The anatomic distribution of the disease varies among the histologic subtypes of HL. Mediastinal involvement is most frequently seen in the nodular sclerosis HL subtype, while splenic involvement is more common in the mixed cellularity HL subtype.[29]

In conclusion, we found that CT findings often allowed differentiation of the various subtypes of PML. HL commonly presents as a mediastinal mass with surface lobulation and involves cervical, mediastinal, hilar, and paraortic nodes. Med-DLBCL demonstrates mediastinal mass without surface lobulation, often associated with vascular involvement, and pleural or pericardial effusion. T-LBL is characterized by mass without surface lobulation involving vascular structures often associated with pleural or pericardial effusion, by systemic nodal involvement including cervical, axillary, paraaortic, mesenteric, and inguinal, and by hepatomegaly and splenomegaly.

REFERENCES

1. Macchiarini P, Ostertag H. Uncommon primary mediastinal tumours. *Lancet Oncol.* 2004;5:107–118.
2. Keller AR, Castleman B. Hodgkin's disease of the thymus gland. *Cancer.* 1974;33:1615–1623.
3. Lazzarino M, Orlandi E, Paulli M, et al. Primary mediastinal B-cell lymphoma with sclerosis: an aggressive tumor with distinctive clinical and pathological features. *J Clin Oncol.* 1993;11:2306–2313.

4. Lichtenstein AK, Levine A, Taylor CR, et al. Primary mediastinal lymphoma in adults. *Am J Med.* 1980;68:509–514.
5. Perrone T, Frizzera G, Rosai J. Mediastinal diffuse large-cell lymphoma with sclerosis. A clinicopathologic study of 60 cases. *Am J Surg Pathol.* 1986;10:176–191.
6. Kirn D, Mauch P, Shaffer K, et al. Large-cell and immunoblastic lymphoma of the mediastinum: prognostic features and treatment outcome in 57 patients. *J Clin Oncol.* 1993;11:1336–1343.
7. Harris NL, Jaffe ES, Stein H, et al. A revised European-American classification of lymphoid neoplasms: a proposal from the International Lymphoma Study Group. *Blood.* 1994;84:1361–1392.
8. Nathwani BN, Kim H, Rappaport H. Malignant lymphoma, lymphoblastic. *Cancer.* 1976;38:964–983.
9. Cossman J, Chused TM, Fisher RI, et al. Diversity of immunological phenotypes of lymphoblastic lymphoma. *Cancer Res.* 1983;43:4486–4490.
10. Weiss LM, Bindl JM, Picozzi VJ, et al. Lymphoblastic lymphoma: an immunophenotype study of 26 cases with comparison to T cell acute lymphoblastic leukemia. *Blood.* 1986;67:474–478.
11. Onishi Y, Matsuno Y, Tateishi U, et al. Two entities of precursor T-cell lymphoblastic leukemia/lymphoma based on radiologic and immunophenotypic findings. *Int J Hematol.* 2004;80:43–51.
12. van Spronsen DJ, Vrints LW, Hofstra G, et al. Disappearance of prognostic significance of histopathological grading of nodular sclerosing Hodgkin's disease for unselected patients. *Br J Haematol.* 1997;96:322–327.
13. Heron CW, Husband JE, Williams MP. Hodgkin disease: CT of the thymus. *Radiology.* 1988;167:647–651.
14. Wernecke K, Vassallo P, Rutsch F, et al. Thymic involvement in Hodgkin disease: CT and sonographic findings. *Radiology.* 1991;181:375–383.
15. Luker GD, Siegel MJ. Mediastinal Hodgkin disease in children: response to therapy. *Radiology.* 1993;189:737–740.
16. North LB, Fuller LM, Hagemeister FB, et al. Importance of initial mediastinal adenopathy in Hodgkin disease. *AJR Am J Roentgenol.* 1982;138:229–235.
17. Bradley AJ, Carrington BM, Lawrance JA, et al. Assessment and significance of mediastinal bulk in Hodgkin's disease: comparison between computed tomography and chest radiography. *J Clin Oncol.* 1999;17:2493–2498.
18. Ha CS, Choe JG, Kong JS, et al. Agreement rates among single photon emission computed tomography using gallium-67, computed axial tomography and lymphangiography for Hodgkin disease and correlation of image findings with clinical outcome. *Cancer.* 2000 15;89:1371–1379.
19. Diederich S, Link TM, Zuhlsdorf H, et al. Pulmonary manifestations of Hodgkin's disease: radiographic and CT findings. *Eur Radiol.* 2001;11:2295–2305.
20. Shaffer K, Smith D, Kirn D, et al. Primary mediastinal large-B-cell lymphoma: radiologic findings at presentation. *AJR Am J Roentgenol.* 1996;167:425–430.
21. Strollo DC, Rosado-de-Christenson ML, Jett JR. Primary mediastinal tumors: Part II. Tumors of the middle and posterior mediastinum. *Chest.* 1997;112:1344–1357.
22. Spiers AS, Husband JE, MacVicar AD. Treated thymic lymphoma: comparison of MR imaging with CT. *Radiology.* 1997;203:369–376.
23. Schwartz EE, Conroy JF, Bonner H. Mediastinal involvement in adults with lymphoblastic lymphoma. *Acta Radiol.* 1987;28:403–407.
24. Chaignaud BE, Bonsack TA, Kozakewich HP, et al. Pleural effusions in lymphoblastic lymphoma: a diagnostic alternative. *J Pediatr Surg.* 1998;33:1355–1357.
25. Press GA, Glazer HS, Wasserman TH, et al. Thoracic wall involvement by Hodgkin disease and non-Hodgkin lymphoma: CT evaluation. *Radiology.* 1985;157:195–198.
26. Cho CS, Blank N, Castellino RA. Computerized tomography evaluation of chest wall involvement in lymphoma. *Cancer.* 1985;55:1892–1894.
27. Bonomo L, Ciccotosto C, Guidotti A, et al. Staging of thoracic lymphoma by radiological imaging. *Eur Radiol.* 1997;7:1179–1189.
28. The International Non-Hodgkin's Lymphoma Prognostic Factors Project. A predictive model for aggressive non-Hodgkin's lymphoma. *N Engl J Med.* 1993;329:987–994.
29. Jaffe ES, Harris NL, Stein H, et al, eds. World Health Organization Classification of tumours. Pathology and genetics of tumours of haematopoietic and lymphoid tissues. Lyon, France: IARC Press, 2001.
30. Addis BJ, Isaacson PG. Large cell lymphoma of the mediastinum: a B cell tumour of probable thymic origin. *Histopathology.* 1986;10:379–390.
31. Davis RE, Dorfman RF, Warnke RA. Primary large-cell lymphoma of the thymus: a diffuse B-cell neoplasm presenting as primary mediastinal lymphoma. *Hum Pathol.* 1990;21:1261–1268.
32. Hoelzer D, Gokbuget N, Digel W, et al. Outcome of adult patients with T-lymphoblastic lymphoma treated according to protocols for acute lymphoblastic leukemia. *Blood.* 2002;99:4379–4385.
33. Ben-Yahuda D, Polliack E, Okon Y, et al. Image-guided core-needle biopsy in malignant lymphoma: experience with 100 patients that suggests the techniques reliable. *J Clin Oncol.* 1996;14:2431–2424.
34. Van Besien K, Kelta M, Bahaguna P. Primary mediastinal B-cell lymphoma: a review of pathology and management. *J Clin Oncol.* 2001;15:1855–1864.

Brief Reports

Transcatheter Arterial Embolization for External Iliac Artery Hemorrhage Associated with Infection in Postoperative Pelvic Malignancy

Yoshitaka Inaba, MD, Yasuaki Arai, MD, Shinichi Ino, MD, Kiyoshi Matsueda, MD, Takeshi Aramaki, MD, and Haruyuki Takaki, MD

Transcatheter arterial embolization was attempted for external iliac artery (EIA) hemorrhage in five patients with wound infection after pelvic malignant tumor surgery. To prevent distal migration of coils and to preserve distal branches of the EIA, the entire weakened artery was occluded with use of coils via a bilateral femoral artery approach with balloon occlusion of the distal side. The success rate was 100%. No limb loss was observed immediately after embolization. This method can prevent distal migration of coils and preserve branches that can be collaterals to the femoral artery, and as such it can be used to embolize an adequate portion of the affected artery.

J Vasc Interv Radiol 2004; 15:283–287

Abbreviations: EIA = external iliac artery, IIA = internal iliac artery

FOR the emergency treatment of arterial hemorrhage in the pelvic region caused by malignant tumor extension or infection developing after tumor resection, transcatheter arterial embolization has recently become preferable to surgical intervention because its hemostatic effect is high and its invasiveness is low (1–6). Embolization of the internal iliac artery (IIA) or its branches is associated with few complications and can be performed relatively easily and safely (1,7). However, because of concern that embolization of the common iliac artery and external iliac artery (EIA) may compromise the circulation of the lower extremities, this procedure must be performed with great care (3–5,8,9). Because of such concerns, there is sometimes hesitation to undertake embolization of these arteries, and embolization may be incomplete in some cases, resulting in recurrence of hemorrhage. The distal and proximal sides of the hemorrhagic site must be adequately embolized, particularly in the presence of infection, because the artery may be extensively weakened, including the portions of the vessel proximal and distal to the pseudoaneurysm (2,6,8,9). At the same time, to maintain blood flow to the lower extremities, branches potentially serving as collateral pathways must be preserved to the extent possible (2,8).

In this study, to preserve such distal branches of the EIA, embolization was prevented from extending further than necessary to the distal side with use of a balloon catheter, and with this embolization method completely isolating the hemorrhagic site up to its proximal side, five cases were treated in which EIA hemorrhage associated with infection developed after malignant tumor surgery. The hemostatic effect of this method and clinical course after embolization were evaluated, and the suitability of this method was considered.

MATERIALS AND METHODS

Patients

Five patients in whom EIA hemorrhage developed after surgery for pelvic malignant tumors at our institution from 1987 to 2001 were treated by transcatheter arterial embolization. This group included two men and three women ranging in age from 40 to 65 years (mean, 54 years). The underlying diseases were rectal cancer (n = 2), recurrence of rectal cancer (n = 2), and recurrence of uterine cervical cancer (n = 1). Three of these patients underwent radiation therapy postoperatively. In all patients, symptoms associated with infection, such as high fever, developed after surgery, and abscess formation was confirmed in four patients 13–85 days (mean, 47 days) after the appearance of infection-induced symptoms. Arterial hemorrhage was confirmed from the drain in four patients and from the vagina in one. In the former four cases, the drain was placed for the abscess, and the period from drain placement until the development of hemorrhage was 12–82 days (mean, 44 days). In all patients, angiography was performed the day the hemorrhage was confirmed, at which time signs of shock were present in three patients. Institutional review board approval was obtained for this study.

Angiographic Findings

Aortography was performed via the femoral artery contralateral to the presumed site of the hemorrhage, fol-

From the Department of Diagnostic and Interventional Radiology, Aichi Cancer Center, 1-1 Kanokoden Chikusa-ku, Nagoya 464-8681, Japan. Received August 22, 2003; revision requested September 26; revision received and accepted November 4. **Address correspondence to** Y.I.; E-mail: 105824@aichi-cc.jp

None of the authors have identified a conflict of interest.

DOI: 10.1097/01.RVI.0000116192.44877.46